

Published in final edited form as:

Biomacromolecules. 2010 November 8; 11(11): 2845–2853. doi:10.1021/bm100526a.

Development of Electrically Conductive Oligo(polyethylene Glycol) Fumarate-Polypyrrole Hydrogels for Nerve Regeneration

M. Brett Runge^a, Mahrokh Dadsetan^a, Jonas Baltrusaitis^c, Terry Ruesink^a, Lichun Lu^a, Anthony J. Windebank^b, and Michael J. Yaszemski^{a,*}

^aMayo Clinic College of Medicine, Departments of Orthopedic Surgery of Biomedical Engineering

^bMayo Clinic College of Medicine, Department of Neurology

^cUniversity of Iowa Central Microscopy Research Facility

Abstract

Electrically conductive hydrogel composites consisting of oligo(polyethylene glycol) fumarate (OPF) and polypyrrole (PPy) were developed for applications in nerve regeneration. OPF-PPy scaffolds were synthesized using three different anions: naphthalene-2-sulfonic acid sodium salt (NSA), dodecylbenzenesulfonic acid sodium salt (DBSA), and dioctyl sulfosuccinate sodium salt (DOSS). Scaffolds were characterized by ATR-FTIR, XPS, AFM, dynamic mechanical analysis, electrical resistivity measurements, and swelling experiments. OPF-PPy scaffolds were shown to consist of up to 25 mol% polypyrrole with a compressive modulus ranging from 265 to 323 kPa and a sheet resistance ranging from 6 to 30×10^3 Ohms/square. In vitro studies using PC12 cells showed OPF-PPy materials had no cytotoxicity and PC12 cells showed distinctly better cell attachment and an increase in the percent of neurite bearing cells on OPF-PPy materials compared to OPF. The neurite lengths of PC12 cells were significantly higher on OPF-PPy_{NSA} and OPF-PPy_{DBSA}. These results show that electrically conductive OPF-PPy hydrogels are promising candidates for future applications in nerve regeneration.

Keywords

hydrogel; electrical; conductive; nerve; tissue regeneration

Introduction

The frequency and disability associated with both spinal cord and peripheral nerve injuries have resulted in a rapidly advancing field to regenerate damaged nerves. The gold standard treatment for segmental nerve loss utilizes autografts, although they have significant limitations, including acquiring adequate lengths and sizes of the necessary donor nerve and misalignment of the complex neurological anatomy that comprises the nerve¹⁻⁴. The combination of these limitations often prevents full functional recovery from a segmental nerve injury. As such, synthetic materials provide an attractive alternative therapy. Synthetic scaffolds can be engineered to possess the desired dimensions, mechanical properties, and degradation profiles. Techniques incorporating stimuli into polymeric scaffolds to stimulate

*Correspondence to: Michael J. Yaszemski, M.D., Ph.D., Mayo Clinic College of Medicine, 200 First Street SW, MS 3-69, Rochester MN 55905, Phone: 507-284-3747, Fax: 507-284-5075, yaszemski.michael@mayo.edu.

Conflicts of Interest

A provisional patent has been filed on oligo(polyethylene glycol) fumarate-polypyrrole based materials, and this technology has been licensed to BonWrx.

nerve regeneration has become increasingly important in this field of research. Stimuli can include topological⁵⁻⁷, biological^{8, 9}, chemical, or electrical cues^{10, 11}.

Electrical stimulation has been gaining increasing attention as studies over the last decade show intermittent electrical stimulation increases neurite and axon extension *in vitro*¹² and nerve regeneration *in vivo*¹³. However, incorporating electrically conductive materials into the biomaterials field remains limited, due to their poor mechanical properties, non-degradability, and difficulty to process into complex three dimensional structures¹⁴⁻¹⁹. Polypyrrole, the most extensively studied electrically conductive polymer for application in nerve guidance conduits, lacks the mechanical properties necessary for robust biomaterial applications. This fact has driven the development of hybrid materials that utilize a host polymer that possesses the desired physical material properties for the bulk composition, while an electrically conductive polymer is a minor component and adds electrical conductive properties to the resulting materials. Recently a number of different polypyrrole composite materials have been developed specifically for nerve regeneration applications. These have included composite materials where the bulk polymer consists of polycaprolactone, poly(lactic-co-glycolic acid), poly(ethyl cyanoacrylate), chitosan, or poly(caprolactone fumarate)^{7, 20-22}. A recent review by Guiseppi-Elie highlights the recent advances in the field of electrically conductive hydrogel composite materials²³. Other potential routes for incorporating electrical conductive properties into biomaterials include the use of conductive nanoparticles or carbon nanotubes, however, they have shown extensive *in vivo* toxicity associated with the size and functional groups of the nanotubes²⁴⁻²⁹.

Recently, we reported the synthesis and fabrication of a composite material consisting of polycaprolactone fumarate (PCLF) and polypyrrole (PPy)³⁰. These materials were interpenetrating networks of PCLF and PPy, and shown to maintain the physical properties of PCLF while adding the electrical conductivity of PPy to the scaffold. In this work, we extend this methodology to the oligo(polyethylene glycol fumarate) (OPF) hydrogel³¹⁻³⁴. OPF hydrogels are synthesized by reaction of fumaryl chloride and polyethylene glycol. The resulting OPF (shown in Figure 1) can be cross-linked by free radical polymerization of the fumarate groups throughout the OPF chain. The cross-linked OPF hydrogel which is insoluble in water allows polymerization of PPy (shown in Figure 1) within its network by means of radical initiation. The chemical synthesis approach to OPF-PPy materials reported here differs from previous hydrogel-PPy composite materials synthesized by electropolymerization techniques. A recent example reported by Justin et al. demonstrated the electropolymerization of pyrrole through poly(hydroxymethylacrylate) based hydrogels³⁵. The resulting materials exhibited a resistance ranging from 5–137 k Ω depending whether PPy was in the oxidized or reduced state. Many previous examples of hydrogel-PPy composite materials have been developed for biosensor³⁵⁻⁴⁰ and neural prosthetic⁴¹⁻⁴⁴ applications. The intended application of the resulting OPF-PPy materials from this study is as nerve guidance conduits. Therefore these materials require significantly larger sizes than an electrode with a thin hydrogel coating as is the case for biosensors and neural prosthetics devices. Additionally, polymeric nerve conduits lack an electrode within the conduit from which pyrrole can be polymerized. Therefore the chemical synthesis of PPy is well suited for the challenges of producing electrically conductive nerve conduits. In fact, other examples using poly(lactic-co-glycolic acid), chitosan, or polycaprolactone fumarate polymeric nerve conduits have used the chemical synthesis approach to incorporate PPy^{7, 14, 21, 22}.

The synthesis of polypyrrole requires the inclusion of anions (Chemical structures shown in Figure 1) that stabilize the positive charge that forms the conductive species of polypyrrole. The three anions used for the synthesis of PPy included naphthalene sulfonic acid, dodecyl

benzene sulfonic acid, and dioctyl sulfosuccinate. These anions were chosen because the resulting PPy materials typically exhibit high conductivity, and previous work has shown they are compatible for biomaterial applications²².

The OPF hydrogel in the OPF-PPy composites is a biodegradable hydrogel that is photo or chemical cross-linkable with tunable material properties through polymer synthesis and cross-linking. Hydrogels are important biomaterials because they are composed of more than 80% water and therefore can closely resemble the physiological environment while allowing nutrient and waste diffusion into or out of the regeneration site. OPF has previously been investigated for multiple tissue engineering applications from drug delivery, to cartilage, to nerve regeneration^{33, 34, 45–48}, and has now been extended to include a conductive polypyrrole composite material. The resulting OPF-PPy composite materials are the first electrically conductive polypyrrole composite hydrogel intended for use as a nerve conduit.

Materials and Methods

Materials

All materials were purchased from Sigma or Fisher and used as is unless otherwise noted.

Fabrication of oligo(polyethylene glycol) fumarate scaffolds

Oligo(polyethylene glycol) fumarate (OPF) was synthesized as previously reported^{32–34}. OPF (1.0 g), N-vinylpyrrolidinone (300 μL) and distilled water (950 μL) were heated gently while mixing. Irgacure 2959 photo-initiator (750 μL at 6 mg mL⁻¹) was added to the OPF solution and vortexed to ensure a homogenous mixture. The solution was poured into glass molds separated by Teflon spacers to form films of 0.5 mm thickness. The OPF was cross-linked by irradiation with UV light ($\lambda = 315\text{--}380\text{nm}$) for 1 hour. OPF hydrogels were then submerged in water overnight to remove residual impurities, and then dried under vacuum. Cross-linked disks of OPF were punched from the film with diameters of 5 mm using a cork borer and used as is.

Synthesis of oligo(polyethylene glycol) fumarate-polypyrrole composite materials

OPF disks were submerged in a solution of benzoyl peroxide (2.0 g, 8 mmol) in 10 mL methylene chloride for 5 min, then dried under vacuum to remove the methylene chloride leaving benzoyl peroxide occluded within the OPF disk. An aqueous solution containing pyrrole (0.4 M) and dodecylbenzenesulfonic acid sodium salt (DBSA) (0.09 M) was cooled to 0°C. The molar equivalent of DBSA was used for the synthesis of other OPF-PPy materials containing dioctyl sulfosuccinate sodium salt (DOSS) or naphthalene-2-sulfonic acid sodium salt (NSA). OPF disks were submerged in the aqueous pyrrole solutions and stirred for 12 hours. The resulting black films were then removed from the aqueous solution, rinsed extensively with water, and swelled in methylene chloride three times and then acetone twice to remove residual impurities. The resulting composite films were subsequently dried and used as is. In this manuscript scaffolds will be referred to as OPF-PPy materials when addressing general properties of the materials, and as OPF-PPy_{anion} when discussing specific polymer samples.

X-ray photoelectron spectroscopy (XPS)

The surface elemental composition of OPF-PPy was characterized on a custom-designed Kratos Axis Ultra XPS system. A complete description of the instrument is given elsewhere⁴⁹. Briefly, the surface analysis chamber is equipped with a monochromated 1486.6 eV aluminum K α source having a 500 mm Rowland circle silicon single crystal monochromator. The typical X-ray gun settings were 15 mA emission current at an

accelerating voltage of 15 kV. Low energy electrons were used for charge compensation to neutralize the sample. Survey scans were collected using the following instrument parameters: energy scan range of 1200 to -5 eV; pass energy of 160 eV; step size of 1 eV; dwell time of 200 ms and X-ray spot size of 700×300 μm. High resolution spectra were acquired in the region of interest using the following experimental parameters: 20 to 40 eV energy window; pass energy of 20 eV; step size of 0.1 eV and dwell time of 1000 ms. The absolute energy scale was calibrated to the Cu 2p_{2/3} peak binding energy of 932.6 eV using an etched copper plate. A magnetic lens, mounted below the sample, combined with the electrostatic lenses, was used to focus the scattered electron beam from the surface. A hemispherical sector analyzer (HSA) was used to analyze the electron kinetic energy, while a delay-line detector measured the electron count.

All spectra were calibrated using the adventitious carbon 1s peak at 285.0 eV. A Shirley-type background was subtracted from each spectrum to account for inelastically scattered electrons that contribute to the broad background. Commercially available CasaXPS software was used to process the XPS data⁵⁰. Transmission corrected relative sensitivity factor (RSF) values from the Kratos library were used for elemental quantification, as implemented into CasaXPS. The components of the peaks contain a Gaussian/Lorentzian product with 30% Lorentzian and 70% Gaussian character. An error of ±0.2 eV is reported for all peak binding energies.

Attenuated total reflectance fourier transform infrared spectroscopy (ATR-FTIR)

The chemical compositions of dry OPF and OPF-PPy composite materials were characterized on a Nicolet 8700 FTIR spectrometer. All spectra were collected using a germanium ATR crystal at a resolution of 4 cm⁻¹ at 1000 cm⁻¹ with a minimum of 64 scans.

Swelling measurements

OPF and OPF-PPy disks were dried under vacuum after fabrication. The dried scaffolds were weighed (W_d) and then submerged in distilled water for 24 hours to allow the hydrogel to equilibrate. The swollen gels were blotted to remove excess water from the surface and weighed (W_s). The swelling ratio was calculated as W_s/W_d, where W_s is the weight after swelling and W_d is the dry weight.

Atomic force microscopy (AFM)

Atomic force microscopy images were taken using Asylum Research MFP-3D instrument. NSC15-AIBS cantilevers from MikroMasch with typical resonant frequency of 315 kHz and typical force constant of 40 N/m were used in all experiments. Samples were fixed to a glass slide by the epoxy glue. Images were acquired in air using alternating current (AC) method.

Surface resistivity

Surface resistivity of PPy-OPF composite materials were measured by placing two gold electrodes on hydrated hydrogel films separated by 0.2 mm. The electrical resistivity was measured with a Fluke 73 multimeter. The sheet resistance was calculated using the equation $R_s = R \times W/L$, where R_s is the sheet resistance, R is the measured resistance, W is the width of the samples, and L is the length between electrodes^{7, 51}.

Compressive modulus

Hydrogels were cast into thin sheets and were swollen in distilled water 24 hours prior to compression testing. Disks of 6.0 × 2.0 mm (diameter × thickness) were punched from swollen films and excess water was blotted dry from the surface. The samples were tested on a TA instruments DMA 2980 in compression mode. The force was ramped from 0–18 N

at a rate of 2 N min^{-1} with a preload force of 0.2 N. The compressive modulus was determined from the linear portion of the stress vs. strain curve between 10 to 20% strain.

Cytotoxicity of OPF-PPy composite materials

PC12 cells (ATCC) were seeded at a density of $20,000 \text{ cells cm}^{-2}$ in 12-well plates 24 hours prior to the addition of hydrogels. PC12 cells were maintained in Dubelco's Modification of Eagle's Medium (DMEM) (Mediatech) supplemented with 10% horse serum, 5% fetal bovine serum, and 0.5% streptomycin/penicillin. Transwells with a mesh size of $8 \mu\text{m}$ containing the hydrogels were placed in the wells with the hydrogels completely submerged in the media. After 1, 3 and 7 days, the transwells containing the hydrogels were removed and the cell numbers were quantified using the MTS assay (CellTiter 96, Promega, Madison, WI) following the manufacturer's instructions.

Attachment of PC12 cells on OPF-PPy materials

OPF-PPy composite materials were fabricated into disks with diameters of 1.1 cm and placed in a 24 well plate. The scaffolds were disinfected in 70% ethanol for 30 minutes and then rinsed several times with sterile PBS. Autoclaved medical grade silicon tubing was inserted into the wells to limit the surface area of the hydrogel disk to a diameter of 0.95 cm with a surface area of 0.71 cm^2 . The well was filled with culture media and incubated for 12 hours to remove any remaining impurities. PC12 cells were plated onto the surface at a density of $30,000 \text{ cells cm}^{-2}$. Experiments were performed with nerve growth factor (NGF) supplemented media at a concentration of 50 ng mL^{-1} . Cell viability was determined using MTS assay (Promega) with the following adjustments. Cells were first trypsinized by adding 1mL trypsin to each well and then aspirating the trypsin followed by incubation at 37°C for 10 min. The cells were gently dislodged from the surface with a cell scraper and transferred to a new well in 0.5 mL media. This step was critical to eliminate any polypyrrole material from transferring as polypyrrole interferes with the MTS assay. Then 0.1 mL of MTS was added to the new well containing the transferred cells and gently mixed. Cells were then incubated for 2 h at 37°C before transferring 100 μL to a 96 well plate. The absorbance was measured at 490 nm on a Molecular Devices Spectramax plate reader.

PC12 cell morphology

Hydrogel disks with PC12 cells were fixed in 2% paraformaldehyde in PBS for 25 min, then washed with PBS three times. Cells were permeablized in 0.1% Triton 100X for 3 min and then incubated in 10% horse serum in PBS for 1 h. Cells were stained in 1% rhodium phalloidin in 5% horse serum in PBS for 1 h and then washed with PBS three times. Disks were stained with DAPI prior to mounting on a glass cover slip. Samples were imaged on an LSM 510 inverted confocal microscope and imaged at an excitation wavelength of 368 and 488 nm. 300 cells were analyzed for neurite extension using the NIH software Image J. Only neurites that were $5 \mu\text{m}$ or longer were counted.

Statistical analysis

Experiments were performed with triplicate specimens and results are reported as means \pm standard deviations. Single factor analysis of variance (ANOVA) was performed (StatView, version 5.0.1.0, SAS Institute, Inc, Cary, NC) to assess the statistical significance of the results. When the global F-test was positive at the 0.05 level, Bonferroni's method was used for multiple comparison tests to determine differences among the experimental groups.

Results

Figure 1 shows chemical structure of OPF and PPy as well as DBSA, NSA and DOSS used as dopants in this study. OPF-PPy materials were synthesized by first fabricating cross-linked hydrogel scaffolds composed of OPF. These scaffolds can be fabricated into complex structures with various dimensions via injection molding followed by photo-cross-linking upon UV exposure. OPF can be photo or chemically cross-linked, however, photo cross-linking yields more consistent results because of the ability to form homogenous mixtures that do not partially cross-link before injection and are completely cross-linked upon UV exposure.

Pyrrole was polymerized in cross-linked OPF by first submerging the OPF scaffolds in a solution of benzoyl peroxide dissolved in methylene chloride. In this step benzoyl peroxide, the initiator for polymerization of pyrrole, diffuses into the OPF scaffold as it swells in the methylene chloride solution. The methylene chloride is then evaporated under vacuum, leaving benzoyl peroxide occluded within the OPF scaffold. These OPF scaffolds loaded with benzoyl peroxide are then submerged in aqueous of pyrrole and the anion. In this step pyrrole and the dopant diffuse into the OPF scaffold as the hydrogel swells in the water. However, benzoyl peroxide does not diffuse out, but remains in the scaffold because it is not soluble in water. Therefore, as pyrrole diffuses into the OPF it is rapidly polymerized by the benzoyl peroxide initiator resulting in OPF-PPy composite materials. These composite materials are composed mainly of OPF. This approach overcomes many synthetic and biological challenges associated with polypyrrole alone; including processing difficulties, poor mechanical properties, and non-biodegradability.

Because OPF-PPy composite materials were cross-linked before synthesizing PPy, final characterization of the OPF-PPy scaffolds relied on ATR-FTIR, XPS, and AFM. After polymerization of pyrrole in OPF, the incorporation of PPy was visually apparent. The OPF scaffold turned from white to characteristic black of PPy and was electrically conductive. OPF-PPy composite materials were first characterized by ATR-FTIR to qualitatively show the presence of PPy in OPF. Figure 2 shows clear peaks present in OPF-PPy materials that are absent in the OPF spectra. An absorption band at 1550 cm^{-1} is characteristic of pyrrole ring skeletal stretches and a strong absorption band present at 750 cm^{-1} is attributed to C-H stretches and overlaps with the S-O stretch from the sulfonate anions that occur from 690–900. In addition, absorption bands present at 1200 cm^{-1} are attributed to C-N stretching, and 1030 cm^{-1} are C-H vibrations⁵².

XPS was used to quantify the atomic composition of the OPF-PPy surface and the results are shown in Table 1 and Figure 3. OPF composition was 73% C, 26% O, and 1% N. The nitrogen incorporation was from copolymerization of OPF with N-vinyl pyrrolidinone, and no N^+ species was detected. OPF-PPy composite hydrogels show large increases in nitrogen composition ranging from 5.07 to 6.34. These percents correspond to PPy incorporation of up to 25 percent into OPF-PPy scaffolds. The N^+ component of PPy can be seen in Figure 3 as the peak at 402 eV. The N^+ component corresponds to the percent of polypyrrole in the electrically conductive state. The typically doping level of polypyrrole ranges from 20–40%⁵³. XPS characterization shows OPF-PPy composite materials incorporated PPy that possess a doping level of 20.0 to 29.4%, which is the range expected for PPy. The XPS data also shows that 1.3 to 1.8 atomic percent sulfur was detected from the anion. These values correlate well with the theoretically expected amount based on 5.07 to 6.34 atomic percent nitrogen and 20 to 29.4 percent doped as indicated by the N^+ species.

The swelling ratios of the hydrogels were compared by measuring the weight increase of the swollen hydrogels and are shown in Table 1. OPF-PPy hydrogels swelling ratios ranged

from 6.4 to 6.8 and all were significantly lower ($p < 0.05$) from 7.8 for OPF. This decrease in swelling is due to the introduction of polypyrrole into the hydrogel matrix. The differences between OPF-PPy_{NSA}, OPF-PPy_{DBSA}, and OPF-PPy_{DOSS} should be affected by the amount of PPy incorporated, but may also be influenced by the anion choice. No significant differences in the swelling ratio between different OPF-PPy groups were observed.

The sheet resistance of OPF-PPy scaffolds were measured by a four point probe and found to range from 6,000 to 33,000 Ω /sq. The measured resistance places these composite materials in the semiconductor range, which is lower than pure polypyrrole, but sufficient for application in biological systems and similar to other composite materials synthesized using polypyrrole^{7, 14, 54} such PPy coated PLGA.

The compressive modulus of OPF and OPF-PPy materials were measured to determine the effect of incorporating PPy on the scaffold mechanical properties and the results are shown in Figure 4. Because hydrogels are composed mostly of water, they generally have a low compressive modulus. OPF was measured to be 191 ± 9 kPa. Incorporation of PPy increased the compressive modulus of the materials by 40–70%, with OPF-PPy_{DBSA}, OPF-PPy_{NSA}, OPF-PPy_{DOSS} increasing to 265 ± 30 kPa, 311 ± 36 , and 323 ± 30 kPa respectively. Statistical analysis showed that all OPF-PPy scaffolds had significantly higher compressive modulus ($p < 0.05$) than OPF, however no significant differences were observed between different OPF-PPy scaffolds.

Figure 5 shows OPF-PPy_{NSA}, OPF-PPy_{DBSA}, and OPF-PPy_{DOSS} scaffold surface topographies characterized by AFM. These scaffolds show the granular structure characteristic of polypyrrole. The granular structures are homogeneously dispersed throughout the scaffold surface and are similar between all samples.

In vitro studies were performed with PC12 cells to test for toxicity and cell attachment to the OPF-PPy materials. Cytotoxicity of leaching material was tested using a non contact cell toxicity experiment where PC12 cells were cultured in polystyrene tissue culture plates and the hydrogels were suspended above the cells via transwells. Cell numbers were analyzed at days 1, 3 and 7 for toxicity from residual materials leaching from the scaffolds and the results are shown in Figure 6. Cells cultured in the absence of hydrogel materials were used as the positive control. No toxicity from any OPF-PPy material was observed.

In vitro studies comparing the cell attachment and proliferation of PC12 cells on tissue culture polystyrene (TCP), OPF-PPy, and OPF materials were also performed. Cell numbers were quantified using the MTS assay (Figure 7). To use the MTS assay the cells were trypsinized from the surface of the OPF-PPy scaffolds to prevent interaction of the hydrogel scaffold with the MTS dye. The formazin dye in MTS contains a negatively charged sulfonate group that can interact with polypyrrole resulting in low absorbance values. Removal of cells from the scaffold before application of the MTS dye solved the problem. The MTS assay shows PC12 cells cultured on OPF-PPy materials are able to attach in equal numbers to the TCP and OPF, with no difference observed between materials at day 1. By day 7, significant differences in the number of cells attached to the different materials can be observed. Fewer cells were observed on OPF materials compared to all OPF-PPy materials. This may have been a result of differences in surface topography as OPF-PPy materials have a granular surface structure. The difference could also be due to differences in chemical composition of the scaffolds.

Morphology and neurite extension from PC12 cells were characterized by fluorescence microscopy. F-actin formation and cytoskeleton organization of PC12 cells were stained with rhodium phalloidin and DAPI was used for nuclei counter staining. Differentiating PC12 cells cultured in the presence of nerve growth factor exhibit neurite extension from the

cell body. Figure 8 shows PC12 cells did not attach well to the surface of OPF. These PC12 cells had round morphologies and did not show extending neurites. However, PC12 cells on OPF-PPy materials had elongated cell bodies with some neurites extending 50 μm or farther from the cell bodies indicative of a differentiating mode.

The neurite extension from PC12 cells after 24 h is quantified in Figure 9a–c. Figure 9a shows the percent of neurite bearing cells, the trend indicates that PPy incorporation increased the percent of neurite bearing cells. PC12 cells cultured on OPF-PPy_{NSA} and OPF-PPy_{DOSS} had 74 ± 1 and 56 ± 7 percent of cells bearing neurites. This is a significant increase ($p < 0.05$) over OPF that had 36 ± 5 percent neurite bearing cells. OPF-PPy_{DBSA} had 50 ± 11 percent and was not significantly higher than OPF, but was significantly lower ($p < 0.05$) than OPF-PPy_{NSA}. Figure 9b shows the average number of neurites per neurite bearing cell. Because the significant difference in the percent of neurite bearing cells, only cells with neuritis were considered to determine the average neurite number. Figure 9b indicates that the trend that PPy incorporation slightly increases average neurite number for all materials. However, only OPF-PPy_{DBSA} shows a significant increase over OPF from 1.5 ± 0.25 to 2.5 ± 0.5 neurites per cell. The PC12 neurite length distribution is shown in Figure 9c. Both OPF-PPy_{NSA} and OPF-PPy_{DBSA} show dramatically different distributions from both OPF and OPF-PPy_{DOSS}. OPF-PPy_{DOSS} and OPF have 79% and 76% of extending neurites shorter than 20 μm , while only 38% and 49% of PC12 neurites cultured on OPF-PPy_{NSA} and OPF-PPy_{DBSA} are shorter than 20 μm . Also, the percent of PC12 cells with 50 μm or longer neurites are 19% and 9% when cultured on OPF-PPy_{NSA} and OPF-PPy_{DBSA}, but only 1.3% and 2.8% when cultured on OPF and OPF-PPy_{DOSS} respectively.

Discussion

Incorporation of electrically conductive materials into tissue engineering approaches, and specifically for nerve regeneration, is a rapidly developing area in tissue engineering. Recently we reported the synthesis of a polycaprolactone fumarate-polypyrrole (PCLF-PPy) composite material that exhibited electrically conductive properties. We also showed improved cell attachment and neurite extension on the surface of these conductive hydrogels. Because of the importance of hydrogels in tissue engineering we used the methodology from the previous work to synthesize an electrically conductive hydrogel for nerve regeneration applications. Hydrogels are a unique class of materials in tissue engineering. Because they are composed mostly of water, they allow diffusion of nutrients through the cross-linked polymeric network, and can mimic the physiological environment.

In this study, OPF based hydrogels were chosen to make PPy composite materials because the material has been thoroughly investigated for application in tissue engineering^{31–34, 46}. One particular analog of OPF is positively charged through incorporation of a quaternary amine that has been shown to increase cell attachment to OPF⁴⁶. This positively charged hydrogel has also been shown to be a promising candidate material for application in spinal cord injury. Although OPF hydrogels contain high percentages of water they do not exhibit any measureable electrical conductivity even when swollen with water. However, combining PPy with OPF produces an electrically conductive hydrogel. This technique allows rapid introduction of polypyrrole into complex three-dimensional scaffolds and overcomes many limitations associated with fabrication of conducting polymers and increases the versatility of incorporating polypyrrole into biomaterials.

XPS characterization shows 5.1 to 6.3 atomic percent nitrogen is present in the final OPF-PPy composite materials. One percent of this was originally present from use of N-vinyl pyrrolidinone used during cross-linking of OPF. Therefore, 4.1 to 5.3 atomic percent

nitrogen is from pyrrole and corresponds to roughly 20.5 to 26.5 mole percent PPy incorporated into the scaffolds.

To determine the effect incorporation of PPy has on the swelling properties of OPF, the swelling ratio of OPF-PPy hydrogels were measured and compared to OPF. The swelling ratio of OPF-PPy hydrogels decreased by 15–20 percent compared to OPF. This decrease is from the hydrophobicity and poor solubility of polypyrrole attributed to the strong pi-pi interactions of polypyrrole. The differences in swelling behavior between OPF-PPy scaffolds is minimal and may be caused by differences in the amount of PPy incorporated into the scaffolds or subtle differences in the anion incorporated. The sheet resistance of OPF-PPy scaffolds was in the range of 6000 to 33000 Ω /sq, which puts these materials in the category of semiconducting materials. The OPF-PPy materials resistance is much higher than that of pure polypyrrole which can be lower 0.1 Ω /sq, however it is in the same range as other PPy composite materials. For instance PPy coated PLGA nanofibers synthesized by Lee et al exhibited a surface resistance of 24,000 Ω /sq, which electrical current was able to be passed through in order to stimulate neurite extension⁷.

The compressive modulus of OPF scaffolds increased after incorporation of PPy. The compressive modulus of hydrogel scaffolds is influenced by the amount of water taken up by the scaffold. Typically the compressive modulus lowers as the percent water taken up increases. Therefore the increase in compressive modulus of OPF-PPy materials from OPF is likely caused by decreased water absorption of OPF-PPy scaffolds compared to OPF, and not from the mechanical properties of polypyrrole itself strengthening the scaffold. The trend in Table 1 and Figure 4 shows that OPF-PPy_{DOSS} scaffolds exhibited the highest modulus and the lowest swelling ratio. OPF-PPy_{DBSA} or OPF-PPy_{NSA} had similar swelling ratios and compressive modulus though no significant differences were observed between different OPF-PPy mechanical properties or swelling ratios.

In vitro studies using PC12 cells were used to evaluate the three OPF-PPy materials with different anions. The different anions were chosen based on the fact that they are commonly used to dope PPy and are important factors in the resulting conductive nature of PPy⁵³. Also, our previous work with PCLF-PPy composite materials synthesized with NSA, DBSA, and DOSS exhibited the most favorable material properties and conductivities²², it therefore seemed logical to start with these three anions because they had favorable interactions in the previous study.

PC12 cells are an immortalized cell line isolated from a neuroendocrine tumor in the rat adrenal medulla⁵⁵. PC12 cells are a good *in vitro* model for neuronal tissue because they stop proliferating and differentiate into the neuronal phenotype upon application of nerve growth factor. Additionally, they are commonly used to evaluate materials for neuronal tissue compatibility and there is vast literature precedence using them. PC12 cells were first used to evaluate cytotoxicity from residual starting materials used in the synthesis of OPF-PPy scaffolds. Potential toxicity can result from residual pyrrole monomer, anions, or benzoyl peroxide used during the polymerization of pyrrole. Extensive purification of the samples by swelling in methylene chloride, acetone, and ethanol was preformed to remove these impurities. After purification no toxicity was exhibited from any OPF-PPy materials.

Secondly, PC 12 cells were used to determine which OPF-PPy hydrogels promote the most favorable cellular response. This information will be important in future studies that pass electrical current through the polymeric scaffolds to stimulate neurite extension. The cellular response of PC12 cells was determined by cellular attachment, proliferation, and neurite extension on OPF-PPy materials and compared to OPF. No clear trend was observed at day 1, but by days 3 and 7, there were clearly less cells attached to OPF than OPF-PPy materials

(Figure 7). This can partly be explained by the poor cell attachment of PC12 cells on OPF which resulted in the removal of cells during media changes throughout the experiment. The morphology of PC12 cells cultured on OPF is shown in Figure 8 and supports this claim. Distinct differences in PC12 cell morphology cultured on different materials can also be seen. PC12 cells cultured on OPF hydrogels show no neurite extension from the cell body, indicating poor cell attachment in response to being cultured on OPF. This can in part be attributed to the high water content of OPF and a hydrated layer on the hydrogel surface that inhibits protein adsorption. Attachment of cells to polyethylene glycol based hydrogels is well documented throughout the literature as being problematic⁵⁶. Incorporation of charged quaternary ammonium salts into OPF hydrogels has been shown to increase cell attachment by changing the surface charge density⁴⁶. Similarly, polypyrrole contains cations along the polymer backbone and the change in surface charge is a likely mechanism for the increased cell attachment to OPF-PPy materials.

Figure 8 shows morphological differences between cells cultured on the various materials. PC12 cells cultured on OPF-PPy_{NSA} or OPF-PPy_{DBSA} hydrogels showed excellent cellular morphologies with increased neurite extension, but neurites were almost non-existent on OPF-PPy_{DOSS} and OPF. Quantification of neurite extension shows trends that OPF-PPy materials promote higher numbers of neurite-bearing cells, more neurites per cell, and longer neurites. PC12 cells cultured on OPF-PPy_{NSA} showed a 2-fold increase over OPF in the percent of neurite-bearing cells. Also, PC12 cells exhibited a 10-fold increase in the percentage of neurites that were 50 μm or longer when cultured on OPF-PPy_{NSA} or OPF-PPy_{DBSA}. PC12 cells cultured on OPF-PPy_{DOSS} had significantly a higher percentage of neurite-bearing cells, however the distribution of lengths of their neurites were very short with most being less than 20 μm . The combination of Figures 7, 8, and 9 indicate that OPF-PPy_{NSA} and OPF-PPy_{DBSA} materials promote PC12 cell attachment and differentiation, however it appears that OPF-PPy_{NSA} is slightly better because it has a significantly higher number of neurite-bearing cells compared to OPF-PPy_{DBSA}. These results agree with a previous study where polycaprolactone fumarate-polypyrrole composite materials using NSA and DBSA anions were shown to promote the most favorable cellular response over other anions³⁰.

Conclusions

Electrically conductive hydrogels were synthesized by polymerizing pyrrole in preformed scaffolds of OPF. OPF-PPy scaffolds were shown to have a composition of 20–25% polypyrrole and have a sheet resistance of 6000–33000 Ω/sq . Incorporation of PPy into OPF decreases the hydrogels swelling ratio up to 20%. The compressive modulus of OPF-PPy scaffolds ranged from 265 to 323 kPa, an increase of 40–70% from OPF. *In vitro* studies show PC12 cells have higher proliferation rate after seven days when cultured on all OPF-PPy materials compared to OPF. In addition, PC12 cells attached and extended longer neurites when cultured on OPF-PPy_{NSA} or OPF-PPy_{DBSA}. This indicates enhanced neuronal differentiation of PC12 cells on these materials. These findings show that OPF-PPy_{NSA} and OPF-PPy_{DBSA} can be appropriate candidates for our future *in vitro* studies involving electrical stimulation.

Acknowledgments

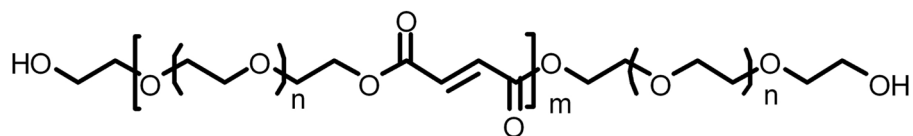
We thank NIH training grant 1T32AR056950-01, the NIH Loan Repayment Program, and the Armed Forces Institute of Regenerative Medicine by DOD activity contract # W81XWH-08-2-0034 for their generous support. We would also like to acknowledge the University of Iowa Central Microscopy Research Facility for XPS characterization.

References

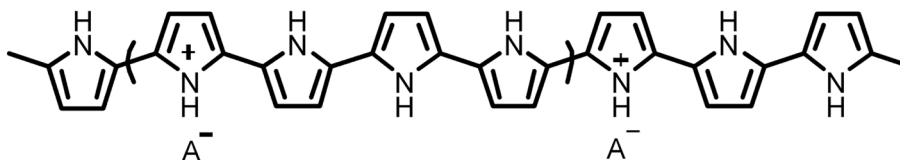
1. Dahlin L, Johansson F, Lindwall C, Kanje M. *Int Rev Neurobiol.* 2009; 87:507–30. [PubMed: 19682657]
2. Colen KL, Choi M, Chiu DT. *Plast Reconstr Surg.* 2009; 124:e386–94. [PubMed: 19952706]
3. Siemionow M, Brzezicki G. *Int Rev Neurobiol.* 2009; 87:141–72. [PubMed: 19682637]
4. Schmidt CE, Leach JB. *Annu Rev Biomed Eng.* 2003; 5:293–347. [PubMed: 14527315]
5. Cao H, Liu T, Chew SY. *Adv Drug Deliv Rev.* 2009; 61:1055–1064. [PubMed: 19643156]
6. Prabhakaran MP, Venugopal JR, Ramakrishna S. *Biomaterials.* 2009; 30:4996–5003. [PubMed: 19539369]
7. Lee JY, Bashur CA, Goldstein AS, Schmidt CE. *Biomaterials.* 2009; 30:4325–4335. [PubMed: 19501901]
8. Arino H, Brandt J, Dahlin LB. *Scand J Plast Reconstr Surg Hand Surg.* 2008; 42:281–285. [PubMed: 18991168]
9. Kemp SWP, Walsh SK, Midha R. *Neurol Res.* 2008; 30:1030–1038. [PubMed: 19079977]
10. Hamid S, Hayek R. *Eur Spine J.* 2008; 17:1256–1259. [PubMed: 18677518]
11. Lu MC, Ho CY, Hsu SF, Lee HC, Lin JH, Yao CH, Chen YS. *Neurorehabil Neural Repair.* 2008; 22:367–373. [PubMed: 18663248]
12. Schmidt CE, Shastri VR, Vacanti JP, Langer R. *Proc Natl Acad Sci USA.* 1997; 94:8948–8953. [PubMed: 9256415]
13. Vivo M, Puigdemasa A, Casals L, Asensio E, Udina E, Navarro X. *Exp Neurol.* 2008; 211:180–193. [PubMed: 18316076]
14. Zhang Z, Rouabhia M, Wang Z, Roberge C, Shi G, Roche P, Li J, Dao LH. *Artif Organs.* 2007; 31:13–22. [PubMed: 17209956]
15. Wang Z, Roberge C, Dao LH, Wan Y, Shi G, Rouabhia M, Guidoin R, Zhang Z. *J Biomed Mater Res A.* 2004; 70:28–38. [PubMed: 15174106]
16. Shi G, Rouabhia M, Wang Z, Dao LH, Zhang Z. *Biomaterials.* 2004; 25:2477–2488. [PubMed: 14751732]
17. Rivers TJ, Hudson TW, Schmidt CE. *Adv Funct Mater.* 2002; 12:33–37.
18. Park JS, Park K, Moon HT, Woo DG, Yang HN, Park KH. *Langmuir.* 2009; 25:451–457. [PubMed: 19049400]
19. Olayo R, Rios C, Salgado-Ceballos H, Cruz GJ, Morales J, Olayo MG, Alcaraz-Zubeldia M, Alvarez AL, Mondragon R, Morales A, Diaz-Ruiz A. *J Mater Sci Mater Med.* 2008; 19:817–826. [PubMed: 17665119]
20. Durgam H, Sapp S, Deister C, Khaing Z, Chang E, Luebben S, Schmidt CE. *J Biomater Sci Polym Ed.* 21:1265–82. [PubMed: 20534184]
21. Huang J, Hu X, Lu L, Ye Z, Zhang Q, Luo Z. *Journal of Biomedical Materials Research - Part A.* 2010; 93:164–174. [PubMed: 19536828]
22. Runge MB, Dadsetan M, Baltrusaitis J, Knight AM, Ruesink T, Lazcano EA, Lu L, Windebank AJ, Yaszemski MJ. *Biomaterials.* 2010; 31:5916–5926. [PubMed: 20483452]
23. Guiseppi-Elie A. *Biomaterials.* 31:2701–16. [PubMed: 20060580]
24. Simon-Deckers A, Loo S, Mayne-L'Hermite M, Herlin-Boime N, Menguy N, Reynaud C, Gouget B, Carriere M. *Environ Sci Technol.* 2009; 43:8423–8429. [PubMed: 19924979]
25. Ji Z, Zhang D, Li L, Shen X, Deng X, Dong L, Wu M, Liu Y. *Nanotechnology.* 2009;20.
26. Pietroiusti A, Iavicoli I, Bergamaschi A, Magrini A. *Int J Environment Health.* 2009; 3:264–274.
27. Dong L, Witkowski CM, Craig MM, Greenwade MM, Joseph KL. *Nanoscale Res Lett.* 2009;1–7. [PubMed: 20652124]
28. Simeonova PP. *Nanomedicine (Lond).* 2009; 4:373–375. [PubMed: 19505238]
29. Belyanskaya L, Weigel S, Hirsch C, Tobler U, Krug HF, Wick P. *Neurotoxicology.* 2009; 30:702–711. [PubMed: 19465056]
30. Runge MB, Dadsetan M, Baltrusaitis J, Knight A, Ruesink T, Lazcano E, Lu L, Windebank AJ, Yaszemski MJ. *Biomaterials.* 2010; 31:5916–5926. [PubMed: 20483452]

31. Temenoff JS, Steinbis ES, Mikos AG. *J Biomater Sci Polym Ed.* 2003; 14:989–1004. [PubMed: 14661875]
32. Shin H, Jo S, Mikos AG. *J Biomed Mater Res.* 2002; 61:169–179. [PubMed: 12061329]
33. Dadsetan M, Szatkowski JP, Yaszemski MJ, Lu L. *Biomacromolecules.* 2007; 8:1702–1709. [PubMed: 17419584]
34. Dadsetan M, Hefferan TE, Szatkowski JP, Mishra PK, Macura SI, Lu L, Yaszemski MJ. *Biomaterials.* 2008; 29:2193–2202. [PubMed: 18262642]
35. Justin G, Finley S, Abdur Rahman AR, Guiseppi-Elie A. *Biomed Microdevices.* 2009; 11:103–15. [PubMed: 18679800]
36. Brahim S, Narinesingh D, Guiseppi-Elie A. *Biosens Bioelectron.* 2002; 17:53–9. [PubMed: 11742735]
37. Abraham S, Brahim S, Ishihara K, Guiseppi-Elie A. *Biomaterials.* 2005; 26:4767–78. [PubMed: 15763256]
38. Abraham S, Brahim S, Guiseppi-Elie A. *Conf Proc IEEE Eng Med Biol Soc.* 2004; 7:5036–9. [PubMed: 17271448]
39. Lingerfelt L, Karlinsey J, Landers J, Guiseppi-Elie A. *Methods Mol Biol.* 2007; 385:103–20. [PubMed: 18365707]
40. Brahim S, Narinesingh D, Guiseppi-Elie A. *Biosens Bioelectron.* 2002; 17:973–81. [PubMed: 12392946]
41. Kim DH, Abidian M, Martin DC. *J Biomed Mater Res A.* 2004; 71:577–85. [PubMed: 15514937]
42. Lee JY, Schmidt CE. *Acta Biomater.*
43. Abidian MR, Corey JM, Kipke DR, Martin DC. *Small.* 6:421–9. [PubMed: 20077424]
44. George PM, Lyckman AW, LaVan DA, Hegde A, Leung Y, Avasare R, Testa C, Alexander PM, Langer R, Sur M. *Biomaterials.* 2005; 26:3511–9. [PubMed: 15621241]
45. Guo X, Park H, Young S, Kretlow JD, van den Beucken JJ, Baggett LS, Tabata Y, Kasper FK, Mikos AG, Jansen JA. *Acta Biomater.* 2009; 6:39–47. [PubMed: 19660580]
46. Dadsetan M, Knight AM, Lu L, Windebank AJ, Yaszemski MJ. *Biomaterials.* 2009; 30:3874–3881. [PubMed: 19427689]
47. Park H, Guo X, Temenoff JS, Tabata Y, Caplan AI, Kasper FK, Mikos AG. *Biomacromolecules.* 2009; 10:541–546. [PubMed: 19173557]
48. Park H, Temenoff JS, Tabata Y, Caplan AI, Mikos AG. *Biomaterials.* 2007; 28:3217–3227. [PubMed: 17445882]
49. Baltrusaitis J, Usher CR, Grassian V. *Phys Chem Chem Phys.* 2007; 9:3011–3024. [PubMed: 17551626]
50. Fairley, N., 2.3.14., C. V., 1999–2008.
51. Tessier D, Dao LH, Zhang Z, King MW, Guidoin R. *Journal of Biomaterials Science, Polymer Edition.* 2000; 11:87–99. [PubMed: 10680610]
52. Hsu CF, Zhang L, Peng H, Travas-Sejdic J, Kilmartin PA. *Current Applied Physics.* 2008; 8:316–319.
53. Skotheim TA, Reynolds JR. 2006
54. Gomez N, Schmidt CE. *J Biomed Mater Res A.* 2007; 81:135–149. [PubMed: 17111407]
55. Greene LA, Tischler AS. *Proc Natl Acad Sci USA.* 1976; 73:2424–2428. [PubMed: 1065897]
56. Holmes PF, Currie EPK, Thies JC, Van Der Mei HC, Busscher HJ, Norde W. *J Biomed Mater Res A.* 2009; 91:824–833. [PubMed: 19051305]

Oligo(polyethylene glycol) fumarate



Polypyrrole



Anions

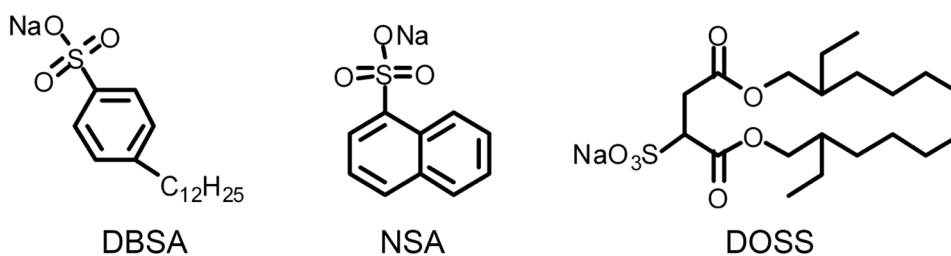


Figure 1. Chemical structure of oligo(polyethylene glycol) fumarate, polypyrrole, and anions dodecylbenzenesulfonic acid sodium salt (DBSA), naphthalene-2-sulfonic acid sodium salt (NSA), and dioctyl sulfosuccinate sodium salt (DOSS) used in the synthesis of OPF-PPy hydrogels.

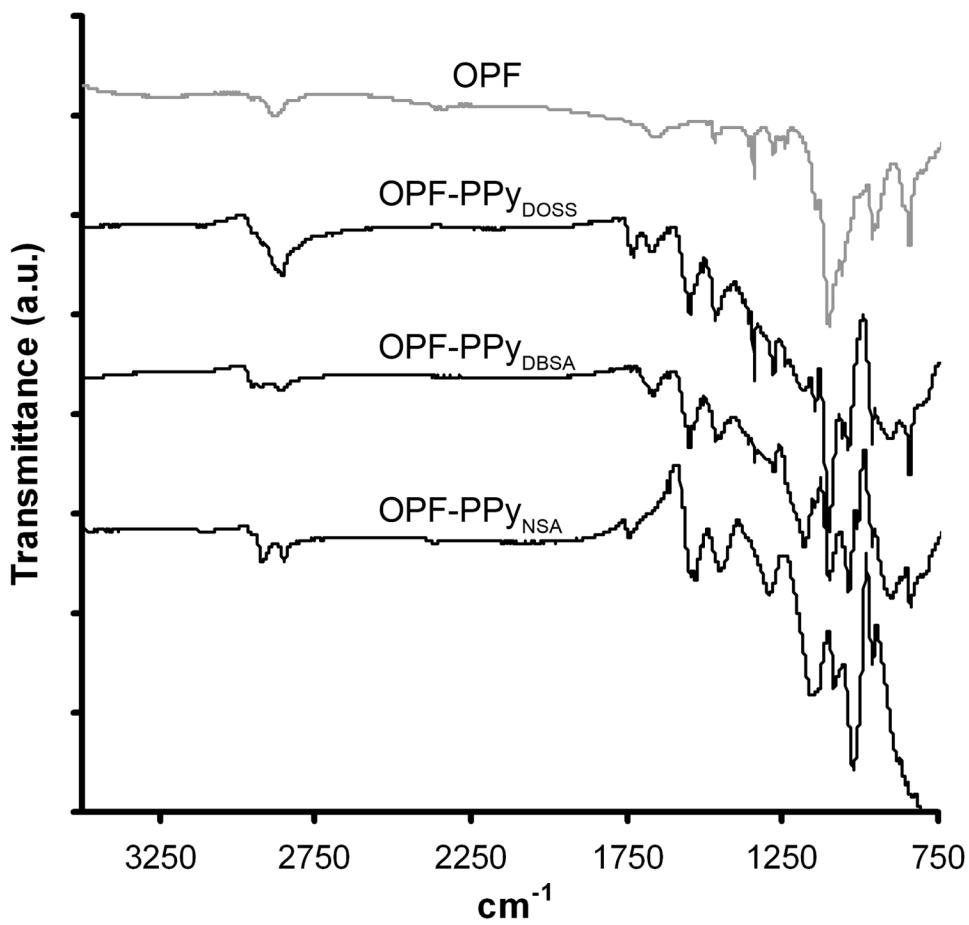


Figure 2. ATR-FTIR of OPF and OPF-PPy materials. Overlapping spectra show the distinct addition of skeletal C-C stretches from polypyrrole at 1550 cm^{-1} and a broad band from $720\text{--}900$ associated with C-H stretches from pyrrole and S-O stretches from NSA.

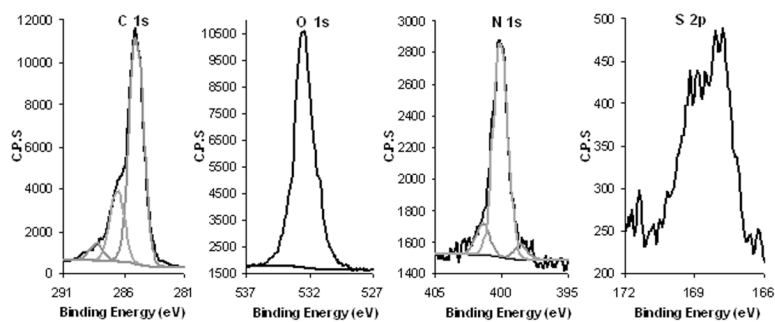


Figure 3. XPS regional scans for C, O, N, and S of OPF-PPy_{NSA}. Regional scan of N show the peak at 402 eV that corresponds to N⁺ species that is the conductive species of polypyrrole.

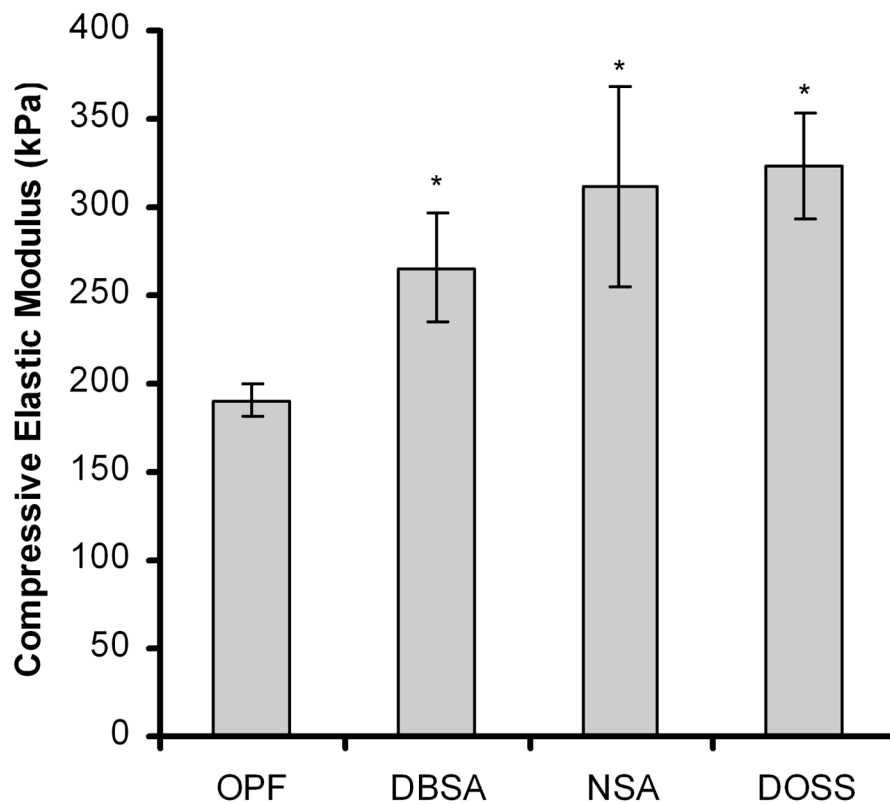


Figure 4. Compressive modulus of OPF and OPF-PPy composite materials synthesized with NSA, DBSA or DOSS anions. Results are reported as means \pm standard deviations, sample size (n=3). *(p<0.05) statistically significant differences of OPF-PPy materials compared to OPF. No statistically significant differences were observed between different OPF-PPy materials.

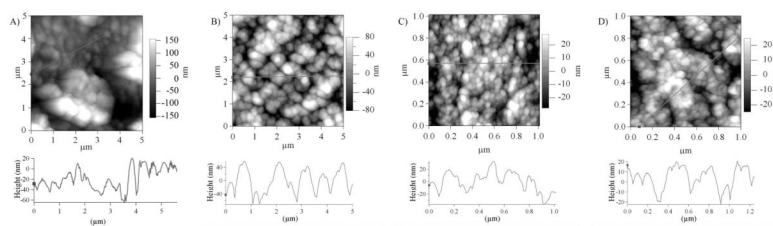


Figure 5. AFM images and corresponding surface profiles of A) OPF B) OPF-PPy_{DBSA}, C) OPF-PPy_{NSA}, D) OPF-PPy_{DOSS}.

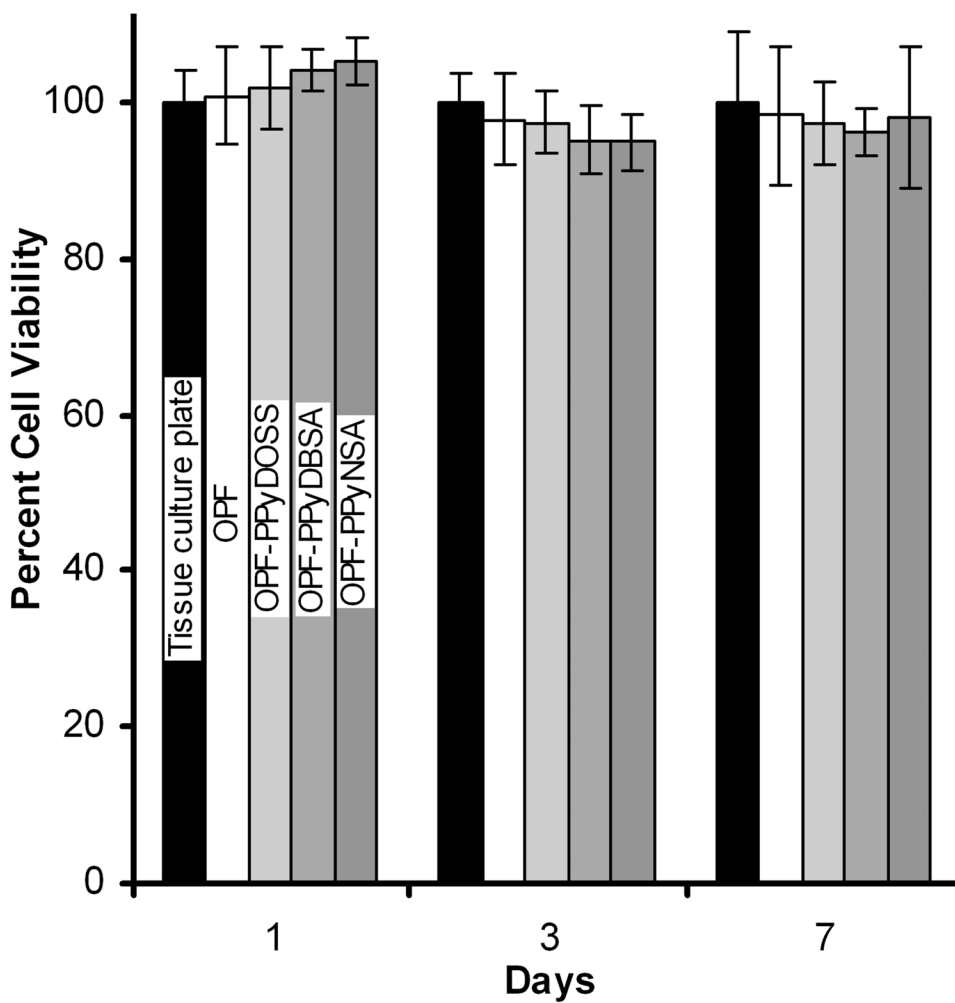


Figure 6. MTS assay evaluating toxicity of potentially leachable materials from OPF-PPy hydrogels. Percent viability was normalized to the tissue culture plate control and values are represented as means \pm standard deviations.

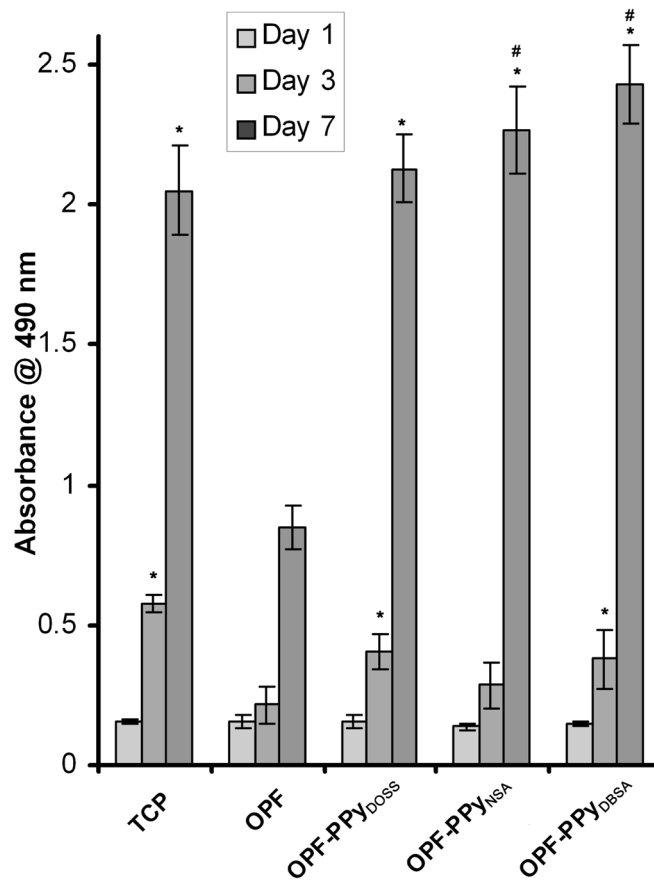


Figure 7.

MTS assay of PC12 indicating cell attachment and proliferation over 7 days. Data are presented as means \pm standard deviations. *($p < 0.05$) significantly higher compared to OPF at the same time point. #($p < 0.05$) significantly higher compared to the tissue culture plate (TCP) at the same time point.

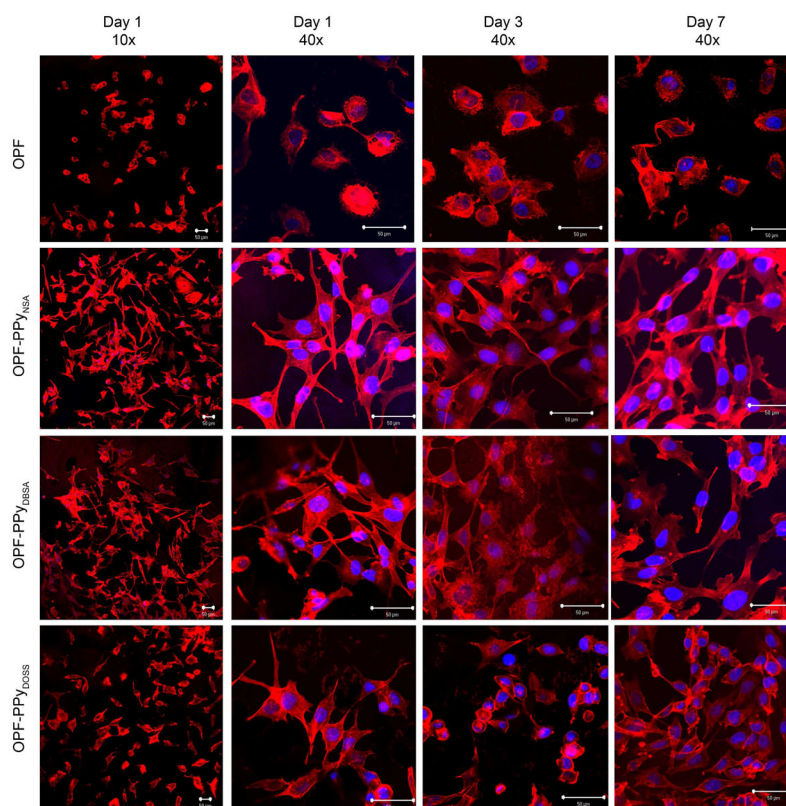


Figure 8. Fluorescence micrographs of PC12 cells at a magnification of 10x or 40x cultured for 1, 3, and 7 days on OPF, OPF-PPy_{NSA}, OPF-PPy_{DBSA}, or OPF-PPy_{DOSS}. All scale bars represent 50 μ m.

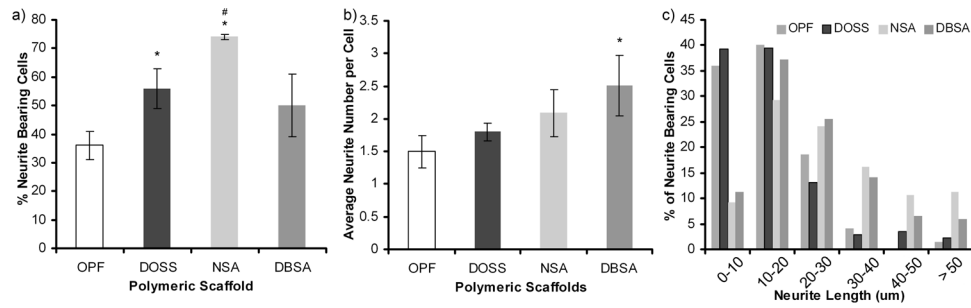


Figure 9. Neurite extension from PC12 cells after 24h quantified as a) percent of neurite bearing cells from the total number of cells. b) average neurite number of neurite bearing cells is shown. c) The distribution of neurite lengths for the OPF and OPF-PPy materials. *($p < 0.05$) Significant difference compared to OPF. [#]($p < 0.05$) Significant difference comparing OPF-PPy_{NSA} and OPF-PPy_{DBSA} materials.

Table 1

	<i>a</i> C	<i>a</i> O	<i>a</i> N	<i>b</i> N ⁺	<i>a</i> S	<i>c</i> S _w /S _d	<i>d</i> R _s (Ω/square)
OPF	73.0	26.0	1.0	0	0	7.8 ± 0.4	NA
OPF-PPy _{DBSA}	79.4	12.5	6.3	20.0	1.8	* 6.7 ± 0.3	6.2 × 10 ³
OPF-PPy _{DOSS}	75.0	17.3	6.3	20.1	1.4	* 6.4 ± 0.4	3.3 × 10 ⁴
OPF-PPy _{NSA}	75.7	17.9	5.1	29.4	1.3	* 6.8 ± 0.3	3.0 × 10 ⁴

^a Atomic composition determined by XPS.

^b Atomic percent of cationic N of total N present in the scaffolds.

^c Swelling ratio of hydrogels determined with distilled water (mean ± standard deviation).

^d Sheet resistance of OPF-PPy scaffolds when swollen with water.

* (p<0.05) significantly different compared to OPF.

No significant differences in swelling ratios were observed between different OPF-PPy materials.